EUROPEAN ACADEMIC RESEARCH
Vol. IX, Issue 12/ March 2022

Impact Factor: 3.4546 (UIF)
DRJI Value: 5.9 (B+)

ISSN 2286-4822
www.euacademic.org

Electrochemistry biosensor for enzymatic activity of G6PD

RONALD RASTRE SALAS
Department of Chemistry, Faculty of Chemistry
Federal University of Amazonas, Amazonas, Brazil
MARCOS MARQUES DA SILVA PAULA
Department of Physic, Faculty of Physic
Federal University of Amazonas, Amazonas, Brazil
WALTER RICARDO BRITO[1]
Department of Chemistry, Faculty of Chemistry
Federal University of Amazonas, Amazonas, Brazil

Abstract

In this work, a biosensor was developed to determine enzymatic activity. This biosensor is based on a specific oxidation/reduction reaction where the glucose-6-phosphate (G6P) substrate is oxidized and the nicotinamide adenine dinucleotide cofactor (NAD+) is reduced by enzymatic catalysis using glucose-6-phosphate dehydrogenase (G6PD). The enzyme was immobilized in DHP on GCE and the electrochemical characterization study was performed using CV and EIE techniques and the surface study was done through SEM, contact angle, and chemical characterization techniques using UV-vis, and SEM-EDS techniques. The analytical curve was performed by DPV that were evaluated in 0.1 mol L^{-1} PBS solution (pH=7.6) with additions of C (NAD^+) $3x10^{-4}$ mol L-1 to different volumes in the electrolyte cell. Linearity was shown from ($7.5x10^{-7}$ to $6.0x10^{-6}$) mol L^{-1} with (R^2 = 0.982), a detection limit (LOD) 1.17 x 10^{-6} mol L^{-1} and quantification limited (LOQ) 1.20 x 10^{-6} mol L^{-1} and an RSD of 6.6% for n=10. The biosensor was shown to be stable for several days.

Keywords: Biosensor; Glucose-6-phosphate; DHP; Glucose-6-phosphate dehydrogenase and NAD^+

1- INTRODUCTION

Malaria is one of the most severe public health problems in the world. It is an infectious disease caused by protozoa of the genus Plasmodium, transmitted

[1] Corresponding author: wrbrito@ufam.edu.br

to humans by female mosquitoes of the genus Anopheles, generating fever and other symptoms. Five Plasmodium species can cause human infections: Plasmodium falciparum, Plasmodium vivax, Plasmodium malariae, Plasmodium ovale, and Plasmodium knowlesi. Among them, Plasmodium falciparum and Plasmodium vivax are the most important species [1]. To treat malaria, many and various drugs containing the 8-aminoquinoline group (such as primaquine, dapsone, and tafenoquine) are used, which are antimalarial drugs commonly used to treat Plasmodium vivax hypnozoites and Plasmodium falciparum gametocytes; However, these medications may cause acute hemolysis in patients with G6PD deficiency [2]. In endemic malaria regions, there is a higher prevalence of G6PD deficiency [3], the rapid discovery of G6PD affectation in patients before the antimalarial drug administer is therefore desirable to minimize the risks for patients who simultaneously have G6PD deficiency.

Glucose 6-phosphate dehydrogenase (G6PD) is a cytoplasmic metabolic enzyme that protects red blood cells from oxidative damage caused by free radicals by limiting oxygen transport. It is estimated that 400 million people worldwide are affected by G6PD deficiency [4], and enzymatic genetic disease that causes fatal hemolysis of red blood cells after exposure to certain medicines and foods [5]. G6PD is part of the phosphate pentose pathway is the first enzyme that catalyzes the oxidation of glucose 6-phosphate (G6P) as substrate and the reduction of coenzyme phosphate nicotinamide adenine dinucleotide ($NADP^+$) and produces a proton **equation 1** [6]. To quantitatively characterize the activity level of G6PD, a routine test uses an ultraviolet spectrophotometer (340 nm) to measure NADPH production in the reaction.

$$\text{Glucose-6-phosphate} + NADP^+ \xrightarrow{G6PD} \text{6-phospho-D-glucono-δ-lactone} + NADPH + H^+ \quad \textbf{(Eq. 1)}$$

In recent years, enzyme-based biosensors have had the advantages of being highly sensitive, fast, accurate, economical, and easy to handle. They can measure specific analytes in complex matrices (such as blood, food, and environmental samples). Many works such as Parelleda in 1998, Fernández in 1998, Bassi in1999, Tzang in 2001, and others authors considering the different combinations of G6PD and different mediators or enzymes, several types of biosensors have been developed, including a series of high-performance biosensors based on the detection of co-substrate consumption or product generation through two enzymatic reactions [4]–[13]. In this work, we present the development of a biosensor to evaluate the enzymatic activity of glucose-6-phosphate dehydrogenase. For this evaluation, the enzyme in Dihexadecylphosphate (DHP) hydrophobic surfactant molecule was immobilized with a negatively charged phosphate group and bound to two long hydrocarbon chains [14], forming a film containing gold nanoparticle

(NPsAu) on the surface of the vitreous carbon electrode (GCE), using as an NAD^+ cofactor and maintaining as substrate G6P.

2- MATERIALS AND METHODS

2.1. Materials

Glucose-6-phosphate dehydrogenase (G6PD) 1mL, Glucose-6-phosphate (G6P), NAD^+ Na 100%, Monobasic and dibasic sodium phosphate (NaH_2PO4/ Na_2HPO4) are obtained from Sigma-Aldrich, Sulphuric acid 98% from Neon, Nuclear isopropyl alcohol, KCl, potassium ferricyanide 99%, and Potassium ferrocyanide 99% from Synth, Dihexadecyl Phosphate (DHP) from Sigma and gold nanoparticles (NPsAu) are obtained from the LABEL research group. All reagents used in the experiments were analytical. The solutions are prepared with Milli-Q Water. The phosphate buffer solution was employed as the supporting electrolyte in all the measurements with the biosensor.

2.2. Equipment

For the performance of electrochemical measurements, potentiostat/galvanostat model PGSTAT204 (Autolab, Metrohm), an electrochemical cell of 3-hole glass with teflon® lid and vitreous carbon electrodes (GCE) in the form of a disc, with a diameter of 3.0 mm, was used platinum wire and Ag/AgCl (3.0 mol L^{-1} KCl) were used as working electrodes, auxiliary and reference electrodes, respectively. All weighings were carried out on analytical scale model AR2140BR (OHAUS) with an accuracy of ± 0.01mg. The pH measurements were performed at pH-equipment model Five Easy F20 (Mettler-Toledo). For stirring the solutions during the voltammetric measurements, the magnetic agitator model NI1107 (Nova) was used and the homogenization of the solutions was performed in an ultrasound bath TS-218 (Dekel). The micrographs were done in the TESCAN Scanning Electron Microscope, vega3a model of the Amazonas National Research Institute. The contact angle was measured with Drop Analysis-LB-ADSA implemented in the ImageJ image processor. UV-VIS spectra are obtained in the Evolution 220 model spectrophotometer (Thermo Fisher Scientific®) using 1 cm buckets in a range of 200 to 900 nm. All experiments are affected at room temperature.

2.3. Preparation of the GCE/ DHP-NPsAu-G6PD biosensor

A glassy carbon electrode (GCE) was carefully polished to a mirror finish with 0.3 and 0.05 µm alumina slurries and rinsed thoroughly with Milli-Q water. The GCE was sonicated in isopropyl alcohol and then with Milli-Q water, each for about 5 min, and taken for electrochemical cleaning in 0.5 mol L^{-1} H_2SO_4, 0.1 Vs^{-1}, 50 cycles using cyclic voltammetry after electrode cleaning dried at room temperature.

A mass of 1.0 mg of DHP was added to 1 mL of (0.1 mol L^{-1}, pH 7.6).Phosphate buffer solution (PBS) and subjected to ultrasonication for 60 min in cool watter to give a dispersion solution. 82.3 µL was collected and were added 11.8 µL of NPsAu 70 ppm and 5.9 µL of G6PD and the mixture ultrasonicated for a further 30 min. Subsequently, 2 µL of this dispersion was cast onto the surface of a GCE and the solvent allowed to evaporate at 25 ± 1◦C for 1h. **Fig. 1** shows the biosensor fabrication process. The GCE/ DHP-NPsAu-G6PD biosensor was stored at 8◦C, when not in use.

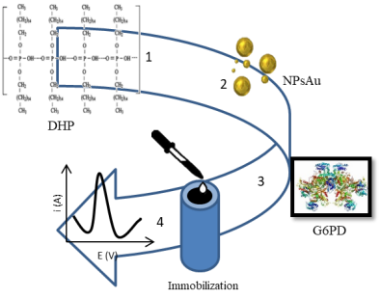

Figure 1 Summary diagram of biosensor preparation

2.4. Electrochemical characterization

The electrochemical evaluations were made for each of the steps that precede the process of immobilization of the G6PD enzyme, and characterization of the biosensor was performed using the techniques of cyclic voltammetry (CV) and electrochemical impedance spectroscopy (EIE). The CV experiments were carried out in buffer phosphate solution 0.1 mol L^{-1} medium containing K_3 $[Fe(CN)_6]$ and K_4 $[Fe(CN)_6]$ 5.0×10^{-3} mol L^{-1} in the range of (-0.4 to 0.8) V to 100 mV s^{-1}. For the use of EIE, the frequency was applied in the interval between 100 Mhz and 100 kHz to 0.1 V with a disturbance amplitude of 10 mV in a previously mentioned medium.

2.5. Analytical procedure

For the development of the analytical methodology, the enzymatic activity of the G6PD was determined under the conditions proposed for the development of the biosensor, by the UV-vis spectrophotometric method, measuring at 340 nm the reduction of the NAD^+/NADH cofactor at different reaction times. Soon the analytical study would continue to determine the optimized conditions of differential pulse voltammetry (DPV) parameters in the following parameters: modulation time 0.02 s, amplitude 25 mV and ΔE 5 mV and time 0.5s in phosphate buffer 0.1 mol L^{-1} and pH 7.6 in the presence of NAD^+ solution ($3x10^{-4}$ mol L^{-1}), G6P (0.2 mol L^{-1}) and Mg^{2+} (0.5 mol L^{-1}), a follow-up performed an electrolyte study varying pH (5.0; 6.8; 7.0; 7.6 and 8.2) of PBS solution. The responses were evaluated by the intensity of peak

currents (Ip), displacement of peak potential, and signal stability after the enzymatic reaction. With the adjusted experimental conditions, the analytical curve was constructed by adding aliquots of the standard NAD^+ solution ($3x10^{-4}$ mol L^{-1}) in the electrochemical cell. The analytical curve was constructed based on the increase of the peak current due to the catalytic activity of the enzyme, which is based on the oxidation of G6P and NAD^+ reduction as shown in **equation 1**. The repeatability tests were performed using nine measurements, using biosensors constructed under the same conditions on the same day. The evaluation was made by calculating the relative standard deviation (%DPR) of the Ip values obtained, according to **equation 2**.

$$\%DPR = \frac{DPI}{Ip} x100 \qquad \textbf{(Eq. 2)}$$

where DPI is the standard deviation of the average of the peak and Ip currents are the average of the peak current values. The measurements were performed in triplicate.

3- RESULTS AND DISCUSSION

3.1. Characterization of the electrode surface

The electroactive area of bare GCE and GCE- DHP-NPsAu was estimated in 0.5 mol L^{-1} KCl in the presence of $5x10^{-6}$ mol L^{-1} $[Fe(CN)_6]^{3-}$ (data not shown) according to the Randles–Sevcik equation 3 [15]:

$$I\,p = 2.69 \times 10^{5}\, AD^{1/2}\, n^{3/2}\, v^{1/2}\, C \qquad \textbf{(Eq.3)}$$

where Ip is the cathodic peak current (A), A is the electroactive area (cm^2), D is the diffusion coefficient of $[Fe(CN)_6]^{3-}$ in solution ($7{,}7 \times 10^{-6}$ $cm^2 s^{-1}$) [16], n is the number of electrons transferred in the redox reaction, v is the potential scan rate (V s^{-1}), and C is the $[Fe(CN)_6]^{3-}$ concentration in bulk solution (mol cm^{-3}). The electroactive areas of the GCE–DHP-G6PD and the bare GCE were calculated to be 0.0534 ± 0.002 cm^2 and 0.06591 ± 0.0004 cm^2 (n = 5), respectively. As shown, there is a decrease in the electroactive area of the electrode with the presence of the polymeric composite involving the enzyme.

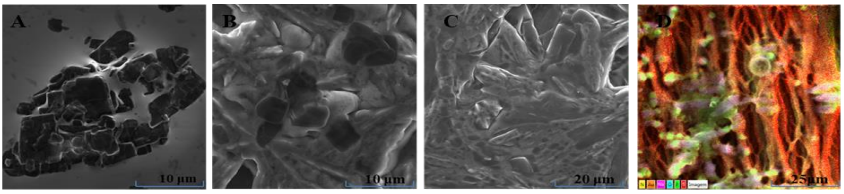

Figure 2. SEM Images of: DHP (A), DHP-NPsAu-G6PD (B) (C) e SEM-EDS (D).

Fig. 2 shows SEM images of DHP, DHP-NPsAu-G6PD, and dispersive energy spectroscopy of the elements on the surface of the GCE electrode. As it is possible to see the film of DHP **Fig. 2A** forms multiple layers, similar to biomembranes probably due to hydrogen bonds [14]. **Fig. 2B-C** is shown as the composite structure sparges over the surface forming many branches with the presence of DHP. **Fig. 2D** shows a color map of the elements found on the superficial: N (yellow), Au (orange), Na (violet), O (blue), P (green), and S (red), corresponding with the chemical structure of the composite. Gold nanoparticles are also observed by ultraviolet spectroscopy (figure not shown).

Table 1 shows the results of wettability (water) referred to the carbon electrode (GCE) and its surface modifications (GCE-DHP, GCE-DHP-NPsAu-G6PD). The results shown have hydrophilic characteristics determined by the values of their contact angles (49.69°; 35.06° and 36.22°) respectively.

Table 1. Contact angle values for modified electrodes

Electrode	GCE	GCE/DHP	GCE-DHP	GCE-DHP-NPsAu-G6PD
Contact angles	49,69	19,83	35,06	36,22

The decrease in the contact angle with respect to GCE can be explained by the hydrophilicity incorporated by the groups: –OH, COOH,=O, vacancies present on the surface of gold nanostructures as well as certain electrostatic interactions present in the enzyme that could favor this fact Fig.3. In the table mentioned above, the GCE contact angle is also shown when a drop of the DHP polymer is placed on the surface of the 19.83° electrode, highlighting its tensioactive characteristics and the affinity of adsorbed by the carbon surface Fig.3B [14].

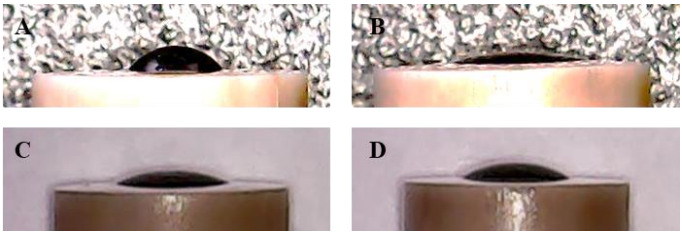

Figure 3. Contact angle of: A) GCE, B) GCE /DHP, C) GCE-DHP, D) GCE-DHP-NPsAu-G6PD.

3.2. Electrochemical characterization of bare GCE and modified GCE

For the development of this project, it was necessary to carry out a preliminary study of the modified carbon electrodes, with thin films of DHP, and involving each of the steps until reaching the final composite developed.

Fig.4A shows the steps of the process characterized by cyclic voltammetry for the carbon electrode and the modified electrode.

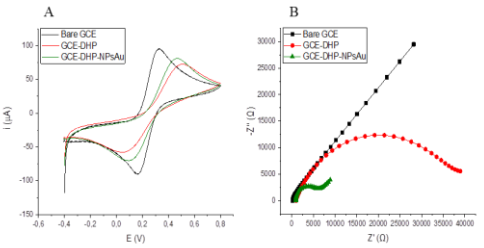

Figure 4. Electrochemical characterization: CV (A) and EIE (B) in PBS (0.1 mol L^{-1}, pH 7.6) containing 5 mmol L^{-1} of $[Fe(CN)_6]^{4-/3-}$, 0.1 V/s.

As observed in Fig. 4A, the bare carbon electrode exhibits a well-defined and reversible response of the made currents of the redox process of the pair $[Fe(CN)_6]^{4-/3-}$, indicating that the electron transfer is controlled by diffusion in the clean electrodes. However, when covering the electrodes with DHP, Ipa decreases by (24.29%) and the Epa (anodic peak potential) moves to ΔEp (0.175) V. This decrease is due to the nature of the resulting film that slows the load transfer, generating repulsions between negatively charged ions when approaching the electrode surface. With the addition of NPsAu, the behavior described above changes and confers on the new composite formed GCE-DHP-NPsAu higher values of peak current 81.2 µA, improving the transfer conditions.

Fig.4B shows the electrochemical impedance study to investigate how the surface of the modified GCE and GCE is affected. Iron-ferricyanide $(Fe(CN)_6)^{3-/4-}$ ion sings as a redox phosphate buffer probe described above. Through the Nyquist graphs shown, one can observe a semicircular part at high frequencies and a linear part at low frequencies that correspond to the limited process of electron transfer and the diffusion process, respectively. The diameter of the semicircle is equal to the load transfer resistance value (Rtc)[17]. Nyquist's experimental data were used to assemble an equivalent circuit model.

As a result, the bare GCE has a lineal profile with load transfer resistance (Rtc) values of $9.33x10^{-3}$ KΩ. The deposition of the DHP molecule on the electrode surface, the Rtc value reaches 142 KΩ; the new layer generates an electrostatic impediment to the anions of the probe in use, thus hindering the diffusion and interaction of the redox pair with the electrode surface and decreasing kinetic velocity of electron transfer [18]. The new modified electrode (GCE-DHP-NPsAu) with gold nanoparticles generates a decrease in the value of Rtc 6.04 KΩ, compared to the DHP film. The new

formation shows a smaller semicircle in the region of high frequencies, which indicates an improvement in load transfer.

3.3. Electrochemical characterization of biosensor

Fig.5 is shown the voltammograms corresponding to the biosensor (GCE-DHP-NPsAu-G6PD) compared with GCE. Fig.5A shows a drop in current, the peak value of anodic current is 29.1 µA which represents a 70% decrease concerning GCE.

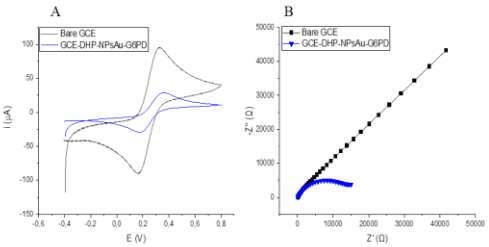

Figure 5. Electrochemical characterization of the biosensor: VC (A) and EIE (B) in PBS (0.1 mol L^{-1}, pH 7.6) containing 5 mmol L^{-1} of $[Fe(CN)_6]^{4-/3-}$, 0.1 V/s.

The incorporation of the biomolecule increases the resistivity of the film with respect to the stages studied during the characterization of modified GCE and GCE. As shown in **Fig.5B**, the new Rtc value for the biosensor was 14.2 KΩ which limits the load transfer speed to the electrode surface.

3.4. Enzymatic activity and enzymatic reaction time

To evaluate the enzymatic activity of the G6PD and define the enzymatic reaction time in the development conditions of the biosensor, a sample was prepared to place 5 µL of the enzyme under study, 20 µL (G6P), 15 µL (NAD^+), 10 µL ($MgCl_2$) and completed up to 2 ml with PBS solution 0.1M pH 7.6. The absorbance reading was performed at times (0; 1; 5; 10; 20; 30; 40; 50; 60) minutes at 340nm at room temperature. One unit of activity (U mL^{-1}) is defined as the amount of enzyme that causes the increase of 0.001 units of absorbance per minute [19], [20].

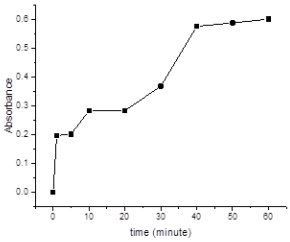

Figure 6. Absorbance measurement in NAD^+/NADH cofactor reduction time.

In **Fig.6** the results indicate that the measurement that the time is eased by the formation of NADH increases, evidenced by the values of absorbances obtained. This situation confirms that the catalytic activity of the enzyme increases as the absorbance of the product increases during the catalytic reaction. The last points of the curve are shown, as the difference between absorbance values decreases due to the existence of fewer NAD^+ molecules to be transformed. For this work, the time of 30 minutes was selected as a time of the enzymatic reaction, due to it being in the central zone of the graph.

3.5. Optimization of the voltammetry parameters of the enzymatic biosensor

Before the construction of the analytical curves for NAD^+, the DPV parameters were optimized in PBS solution 0,1 mol L^{-1}, pH 7.6. Modulation time was investigated in the range of (0.01 to 0.05) s being 0.02s as optimized value, amplitude (25 to 150) mV reaching 25 mV, as adequate value, and ΔE (2.5 to 100) mV, exhibiting 5 mV as optimized. The response was evaluated taking into account the current intensity values and details of the Fig.7 voltammogram, with the addition of 20 µL (G6P), 20 µL (NAD^+), 10 µL ($MgCl_2$).

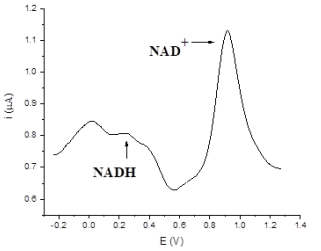

Figure 7. DPV of the biosensor GCE-DHP-NPsAu-G6PD Vs 20 µL (NAD^+) in PBS 0,1 mol L^{-1} pH 7,6 solution.

Fig.7 shows the current peaks of the oxidation and reduction process of the NAD^+/NADH molecule obtained by the DPV method. NADH formation is an indicator of the occurrence of enzymatic catalysis. As shown in the voltammogram, the current peaks corresponding to NAD^+/NADH were identified in the potentials +0.91 and +0.03 volts, respectively, referring to the oxidation/reduction processes. The increase in the reduction current is related to the greater formation of NADH, which in turn holds a close relationship as the largest amount of active enzyme centers available to accelerate the oxidation of G6P molecule, natural substrate of the enzymatic reaction.

3.6. Influence of pH of the support electrolite on the activity of the G6PD

After optimizing the parameters of the use technique, the effect of the pH of the medium on the response of the device was performed. The experiments were carried out for 20 µL (NAD^+) of $3x10^{-4}$ mol L^{-1} as standard solution in phosphate buffer solution 0.1M, pH 7.6.

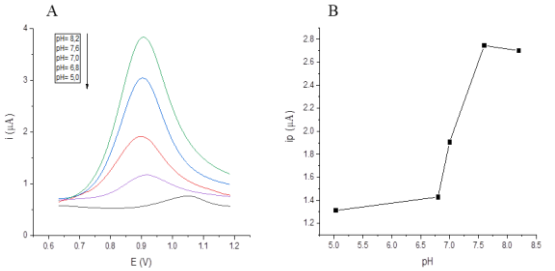

Figure 8. DPV pH effects on NAD^+ (A) and G6PD biosensor response (B) in PBS 0.1 mol L^{-1}, pH 7.6.

The results of the study are shown in **Fig.8** obtaining a better peak current signal for pH 8.2 of the oxidized form NAD^+, but did not correspond with the maximum peak current value of reduction of NADH formation. The enzymatic reaction is favored according to literature at pH close to 7.8, with 7.6 pH value with the highest peak of reduction current intensity [21]–[23].

3.7. Construction of analytical curves for NAD+

The analytical curve was constructed using the method of addition of standards. Aliquots of (5 to 40) µL of NAD^+ of $3x10^{-4}$ mol L^{-1} to the electrochemical cell, with agitation for 3 seconds and incubation time for the reaction of enzymatic catalysis of 30 minutes. The readings were performed in triplicate using the DPV technique in PBS solution 0.1 mol L^{-1}, pH 7.6.

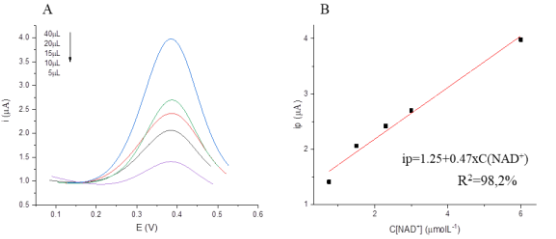

Figure 9. DPB: analytical curve of biosensor response before different additions NAD^+ (A) and correlation of the response obtained (B).

Fig. 9 show voltammogram obtained and the analytical curve (inset) for NAD+ using the proposed GCE-DHP-NPsAu-G6PD biosensor. The DPV

method showed a linear response to NADH in the concentration range from (7.5×10^{-7} to 6.0×10^{-6}) mol L^{-1}, following the equation Ip (μA) = 1.25 +0.47 ×C (mol L^{-1}) with a correlation coefficient of 0.982. The limit of detection (three times the standard deviation for the blank solution (n = 10) divided by the slope of the analytical curve) was calculated as 1.17×10^{-6} mol L^{-1} and the limited of quantification was calculated as 1.20 x 10^{-6} mol L^{-1}. Pearson's coefficient of variation was 6.6% considered low.

3.8. Biosensor stability

The biosensor stability assays (**Fig.10**) were performed by analyzing the Ip values for NAD^+ $3x10^{-4}$ mol L^{-1} in PBS 0,1 mol L^{-1} pH 7.6, from the DPV experiments, carried out on different days.

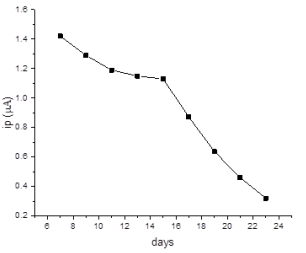

Figure 10. Biosensor stability study

The results indicated that after 23 days the response of the biosensor became 8 % of the initial response. Studies presented in the literature have not shown stability assays of G6PD-based biosensors in the range of 5 to 20 days, with significant loss of enzymatic activity.

4- CONCLUSIONS

From the results obtained, it can be concluded the electrochemical biosensor based on the Enzyme G6PD was successfully applied to the determination of enzyme activity based on the production of NADH in synthetic samples. Using the encapsulation method, G6PD was adequately immobilized on modified GCE with gold nanoparticles and DHP, potentiating the application of the device for analysis. The developed device showed excellent sensitivity in the following conditions: 5.9 μL of the enzyme, 30 minutes of incubation, phosphate buffer 0.1 mol L^{-1}, pH 7.6 and PVD parameters (tm= 0.02 s, a = 25 mV and ΔE = 5 mV). The LOD and LOQ values calculated were 1.17×10^{-6} and 1.20 x 10^{-6} mol L^{-1}, respectively. Stability tests indicated that the biosensor response after 23 days was 8% of the initial response. Therefore, this electrochemical device based on the G6PD enzyme presented desired analytical performance to determine the activity of G6PD, aiming at the

development of a future amperometric sensor for the detection of enzymatic deficit of G6PD in real samples. The biosensor is easy to build, has satisfactory sensitivity, adequate working range, 6.6% DPR in repeatability conditions, and stability. The biosensor has the coverage of unfolding in the future for G6P analyses in different medium environmental samples.

Acknowledgements
The authors deeply thank Capes, CNPQ, FAPEAM and all persons and institutions for the economic support during this investigation.

BIBLIOGRAPHY

[1]B. M. da S. S. de V. em Saúde, "Manual de diagnóstico laboratorial da malária," Brasil, 2009. [Online]. Available: https://bvsms.saude.gov.br/bvs/publicacoes/manual_diagnostico_laboratorial_malaria_2ed.pdf.
[2]C. I. Fanello *et al.*, "High Risk of Severe Anaemia after Chlorproguanil_Dapsone+Artesunate Antimalarial Treatment in Patients with G6PD (A-) Deficiency," *plos aone*, vol. 3, no. 12, p. 4031, 2008, doi: https://doi.org/10.1371/journal.pone.0004031.
[3]E. B. E.T. Nkhoma, C. Poole, V. Vannappagari, S.A. Hall, "The global prevalence of glucose-6-phosphate dehydrogenase deficiency: a systematic review and meta-analysis," *Blood Cells Mol.Dis*, vol. 42, no. 3, pp. 267–278, 2009, doi: https://doi.org/10.1016/j.bcmd.2008.12.005.
[4]A. . Bassi, D. . Tang, and M. . Sergougnou, "Mediated, amperometric biosensor for glucose-6-phosphate monitoring based on entrapped glucose-6-phosphate dehydrogenase, Mg+2 íons, tetracyanoquinodimethane, and nicotinamide adenine dinucleotide phosphateincarbonpaste," *Anal. Biochem.*, vol. 268, no. 2, pp. 223–228, 1999.
[5]J. Parellada *et al.*, "Imunossensores amperométricos e eletrodos de enzima para aplicações ambientais," *Anal. Chim. Acta*, vol. 362, pp. 47–57, 1998.
[6]R. C. H. Kwan, P. Y. T. Hon, W. C. Mak, L. Y. Law, J. Hu, and R. Renneberg, "Biosensor for rapid determination of 3-hydroxybutyrate using bienzyme system," *Biosens. Bioelectron.*, vol. 21, no. 7, pp. 1101–1106, 2006, doi: https://doi.org/10.1016/j.bios.2005.04.005.
[7]Y. Cui, J. P. Barford, and R. Renneberg, "Amperometric Determination of Phosphoglucomutase Activity with a Bienzyme Screen-printed Biosensor," *Anal. Biochem.*, vol. 354, no. 1, pp. 162–164, 2006, doi: https://doi.org/10.1016/j.ab.2006.03.045.
[8]J. Fernández, J. López, X. Correig, and I. Katakis, "Biossensores de fosfato de pasta de carbono sem reagente: estudos preliminares," *Sensores Actuators B*, vol. 47, pp. 13–20, 1998.
[9]C. H. Tzang, R. Yuan, and M. Yang, "Biossensores voltamétricos para a determinação de formato e glicose-6-fosfato com base na medição de NADH e NADPH gerados por desidrogenase," *Biossensores e bioeletrônica*, vol. 16, no. 3, pp. 211–219, 2001, doi: https://doi.org/10.1016/S0956-5663(00)00143-3Obtenha direitos e conteúdo.
[10]M. Skoog, F. Scheller, A. Bückmann, and G. Johansson, "Reagentless enzyme electrode for glucose-6-phosphate using a mediator-modified graphite electrode and macromolecular NAD+," *J. Biotechnol.*, vol. 20, no. 2, pp. 181–188, 1991, doi: https://doi.org/10.1016/0168-1656(91)90226-L.
[11]R. Iyer, V. Pavlov, I. Katakis, and L. G. Bachas, "Amperometric Sensing at High Temperature with a 'Wired' Thermostable Glucose-6-phosphate Dehydrogenase from Aquifex aeolicus," *Am. Chem. Soc.*, vol. 75, no. 15, pp. 3898–3901, 2003, doi: https://doi.org/10.1021/ac026298o.
[12]F. Mazzei, B. Francesco, and C. Botrè, "Acid phosphatase/glucose oxidase-based biosensors for the determination of pesticides," *Anal. Chim. Acta*, vol. 336, no. 1–3, pp. 67–75, 1996, doi: https://doi.org/10.1016/S0003-2670(96)00378-9.
[13]S. Suye, H. Okada, T. Hori, and H. Zheng, "Assembly of alternating polymerized mediator, polymerized coenzyme, and enzyme modified electrode by layer-by-layer adsorption technique,"

Sensors Actuators B Chem., vol. 108, no. 1–2, pp. 671–675, 2005, doi: https://doi.org/10.1016/j.snb.2004.11.090.
[14]B. C. Janegitz *et al.*, "The use of dihexadecylphosphate in sensing and biosensing," *Sensors Actuators, B Chem.*, vol. 220, pp. 805–813, 2015, doi: 10.1016/j.snb.2015.06.020.
[15]A. J. . BARD and L. R. FAULKNER, "Fundamentals and Applications," in *ELECTROCHEMICAL METHODS*, 2nd ed., New York: John Wiley & Sons, Inc, 2001.
[16]J. E. BAUR, "Diffusion Coefficients," in *Handnook of Electrochemistry*, São Paulo: Elsevier Inc., 2007, pp. 845–847.
[17]J. Wang, *Analytical Electrochemistry*, 2nd ed. Hoboken, NJ, USA: John Wiley & Sons, Inc., 2006.
[18]A.-E. Radi, X. Muñoz-Berbel, V. Lates, and J.-L. Marty, "Label-free impedimetric immunosensor for sensitive detection of ochratoxin A," *Biosens. Bioelectron.*, vol. 24, no. 7, pp. 1888–1892, 2009, doi: https://doi.org/10.1016/j.bios.2008.09.021.
[19]O. Fatibello-Filho and I. da C. Vieira, "USO ANALÍTICO DE TECIDOS E DE EXTRATOS BRUTOS VEGETAIS COMO FONTE ENZIMÁTICA," *Quim. Nova*, vol. 25, no. 3, pp. 455–464, 2002, [Online]. Available: https://www.scielo.br/j/qn/a/W3bLHsLZzBYVzhHCRXqnGCQ/?format=pdf&lang=pt.
[20]K. O. Lupetti, L. A. Ramos, and O. Fatibello-Filho, "Determinação enzimática de dopamina em formulações farmacêuticas utilizando sistema de análise por injeção em fluxo com extrato bruto de abacate (Persea americana)," *Quim. Nova*, vol. 26, no. 2, pp. 197–201, 2003, doi: https://doi.org/10.1590/S0100-40422003000200010.
[21]A. Ishaque, M. Millhausen, and H. . Levy, "On the absence of cysteine in glucose-phosphate dehydrogenase from Leuconostoc mesenteroides," *Biochem. Comm*, vol. 59, p. 894, 1974.
[22]C. Olive and H. . Levy, "Glucose-6-phosphate dehydrogenase from Leuconostoc mesenteroides," *Methods Enzym.*, vol. 41, p. 196, 1975.
[23]P. Rowland, A. K. Basak, S. Gover, H. . Levy, and M. . Adams, "The threedimensional structure of glucose-66-phosphate dehydrogenase from leuconostoc mesenteroides refined at 2.0 A resolution," *Structure*, vol. 2, no. 11, pp. 1073–1087, 1994.